Preparation and Optical Properties of Silver Nanoparticle-Polymer Composite Films
銀ナノ粒子—高分子複合膜の作成と光学特性

Shizuyasu Ochiai †, Yu Zhang††, Yoshiyuki Uchida†, Asao Ohashi † and Kenzo Kojima †
落合　鎮康，張　宇，内田 悦行，大橋 朝夫，小嶋 憲三

Abstract: Ag colloid self-assembled films (colloidal metal films) including monolayer (glass/(PVP_d-nanoAg)$_1$) and multilayer (glass/(PVP_d-nanoAg)$_n$) were fabricated by layer-by-layer self-assembly method, where PVP_d (poly(4-vinylpyridine)) was used to link metal nanoparticles by metal-ligand interactions. The obtained monolayer and multilayer films are optically stable at ambient environment, as demonstrated by absorption spectrum measurements. The plasmon resonance of isolated Ag nanoparticles (individual plasmon resonance) and collective plasmon resonance (interparticle plasmon resonance) were observed simultaneously for both mono- and multilayer films. And the intralayer collective resonance in the monolayer films and the interlayer collective resonance in the multilayer films have been investigated and distinguished experimentally. The influence of the post-treatment processes, including drying from different solvents and heating at a higher temperature, on the collective resonance was also evaluated. It is found that the heating treatment and washing with solvents of different surface tension is able to modify the collective resonance of Ag nanoparticles in the films.

1. Introduction

Metal nanoparticles have been the subject of extensive research for many years because of their prominent electromagnetic properties originating from the resonance interaction between light and collective conduction electron oscillations, so-called surface plasmon[1,2]. It has been shown that, by varying the particle shape, size, and spacing, the surface plasmon resonance (SPR) peak can be tuned in a wide range of wavelengths[3-5]. On the other hand, changing the environment and the level of the nanoparticles aggregation (distance and locations) can significantly affect the optical properties of matrix-nanoparticle composites[6-8]. Thus, embedding the metal nanoparticles into organic-inorganic assemblies can be used to either tune their optical properties[9-11]. To date, several nanofabrication techniques have been applied for the construction of the metal nanoparticle-organic films including the most widely used Langmuir-Blodgett deposition[12,13], chemical self-assembly[14], and electrostatic layer-by-layer (LbL) assembly[11]. Those techniques provided organized molecular films with regular multilayered structures from a variety of polymeric and organic molecules[15,16]. The gold nanoparticle-polyelectrolyte multilayer superlattices with tunable optical properties have been fabricated with the LbL technique[17,9]. In these condensed, organized films, the gold nanoparticles embedded in an organic matrix with very different dielectric properties are subject to strong interaction with this matrix and with each other within and between individual layers.

In this paper, we mainly present Ag colloid self-assembled films (colloidal metal films) including monolayer (glass/(PVP_d-nanoAg)$_1$) and multilayer (glass/(PVP_d-nanoAg)$_n$) which were fabricated by layer-by-layer self-assembly method, where PVP_d (poly(4-vinylpyridine)) was used to link metal nanoparticles by metal-ligand interactions. Their structures and optical properties were also characterized and studied experimentally. In particular, we focus on the influence of nanoparticle aggregation and dielectric environment on the plasmon resonance of Ag nanoparticles.

†　愛知工業大学　工学部　電気学科（豊田市）
††　Southeast University Key Laboratory of Molecular and Boimolecular Electronics,Ministry of Education (Nanjing 210096, P. R. China)

2. Experimental

2.1 Chemicals

Silver nitrate, $AgNO_3$ (99.9%) was used as precursor of Ag nanoparticles. Sodium citrate was used as a reducing agent. Both were purchased from Wako Pure Chemical Industries, Ltd. Poly(4-vinylpyridine) (PVP_d, MW160 000) was purchased from Aldrich. Ethanol (EtOH, 99.5%) (Amakasu) was used as solvents. All of the chemicals were used as received from the suppliers. Water used in all experiments was ultrapure 18 MΩ water from Milli-Q water system (Millipore).

2.2 Chemical preparation of Ag nanoparticle colloid[18]

Silver colloid was prepared by rapid addition of a reducing agent of sodium citrate (1% mass concentration, 10 ml aqueous solution) into an aqueous solution of $AgNO_3$ (0.88 mM) which had been heated to 95 °C by water bath and stirred vigorously. Here sodium citrate also acts as stabilizer of nanoparticles. After the reaction was carried out for 45 min, it was stopped and a greenish yellow silver colloid was obtained. Prior to use, the silver colloid was aged overnight.

Self-assembly of Ag nanoparticle monolayer on glass surface by PVP_d (poly (4-vinylpyridine)) linking

Glass coverslips were used as substrates for the deposition of PVP_d film. Prior to the deposition, glass coverslips were cleaned for 15 min in freshly prepared 1:3 mixture of 30% H_2O_2 and H_2SO_4 (piranha solution) followed by washing with ultrapure water and dying at room temperature.

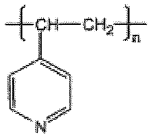

Figure 1. Structural formula of poly (4-vinylpyridine).

Poly (4-vinylpyridine) (Mw=160,000) (Aldrich) was used as received (Figure 1). The polymer was dissolved in reagent alcohol and the solution was used for the deposition of polymer film on glass substrates by adsorption. PVP_d is an efficient surface modifier for immobilization of metal nanoparticles because it is capable of simultaneous interaction with various substrates via hydrogen bonding and with metal particles through metal-ligand interactions of the nitrogen atom on the pyridyl group[19].

Typically, PVP_d-modified glass coverslips (called as glass/PVP_d) were prepared by immerging the cleaned glass coverslips in 0.5% PVP_d in ethanol for one hour. After that, the glass coverslips were washed with ethanol thoroughly and then annealed at 120 °C for 3 h.

The Ag nanoparticles were self-assembled into two-dimensional (2D) arrays by immerging the PVP-modified glass coverslips in the Ag colloid for one hour, and then the obtained films (named as glass/PVP_d-nanoAg) were washed with ultrapure water thoroughly and finally with ethanol followed by drying at room temperature. The obvious pale green color for the films could be observed. In order to increase the density of Ag particles in films, prolonged immerging time (7 and 24 hours) was adopted. With increasing the immerging time, the green color of colloidal Ag films gradually become more obvious. The obtained three samples were marked as 1#, 7#, and 24#, respectively.

2.3 Deposition of alternating multilayer films of glass/(PVP-nanoAg)$_n$ by adsorption cycles

The glass/(PVP_d-nanoAg)$_n$ (n=1,2,3,4) multilayer films were fabricated by alternating and sequential adsorption of PVP and Ag nanoparticles from the corresponding solutions with intermediate thorough washing with ethanol and water. The structure of the multilayer films can be expressed as,

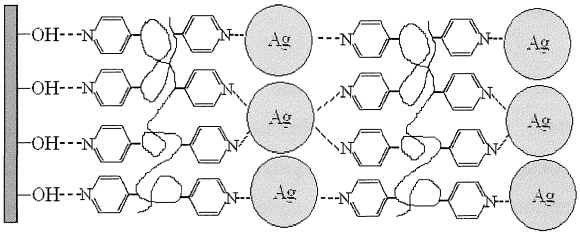

(Figure 2)

Figure 2. Schematic structure of glass/(PVP_d-nanoAg)$_n$ multilayer film

The total four cycles were carried out and the green color of the obtained films gradually become deep. The finally obtained sample of glass/(PVP_d-nanoAg)$_4$ is marked as M#.

2.4 Characterization Techniques

UV-vis spectra were recorded using a UV-2450 UV-visible spectrophotometer (Shimadzu). Atomic force microscope (AFM, OLYMPUS NV-2000) was used to observe the morphology of films.

3. Results and discussion

3.1 AFM observation

The morphology of Ag nanoparticles in films was observed by AFM. Figure 3 gives the AFM images of the samples 1#, 7#, 24#, and M# in a scan range of 10×10μm. It can be seen that Ag nanoparticles in films aggregated into clusters and the density of which on the film surfaces increased with immerging time. From a few aggregated Ag nanoparticle chains observed in the sample of 1#, the diameter of Ag nanoparticles could be estimated to be 50-60 nm. Note that, the Ag nanoparticle clusters seem to gradually become small and compact with increasing immerging time. For the sample of 1#, the average transverse width of the Ag particle clusters was estimated to be 250-500 nm and their height in z direction to be less than 100 nm according the z scale. From these assessments, it is believed that the Ag nanoparticle clusters have an oblate shape, due likely to the interaction between Ag nanoparticles and PVP_d on substrate surfaces. Such cluster morphology can be seen more clearly from an amplified image for the sample 1# (Figure 4). For the sample of M#, the morphology is similar to that of the sample of 7#.

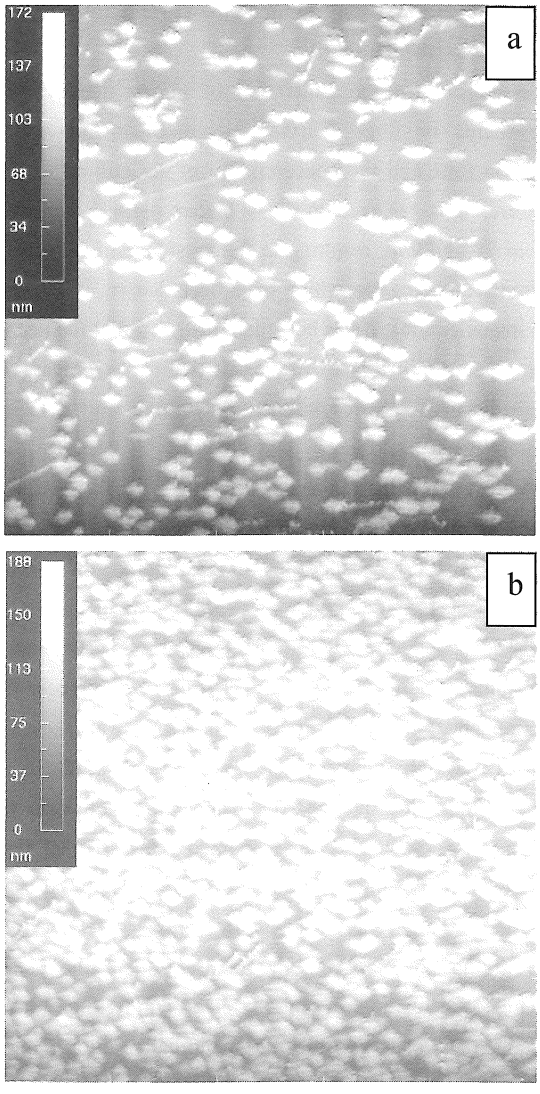

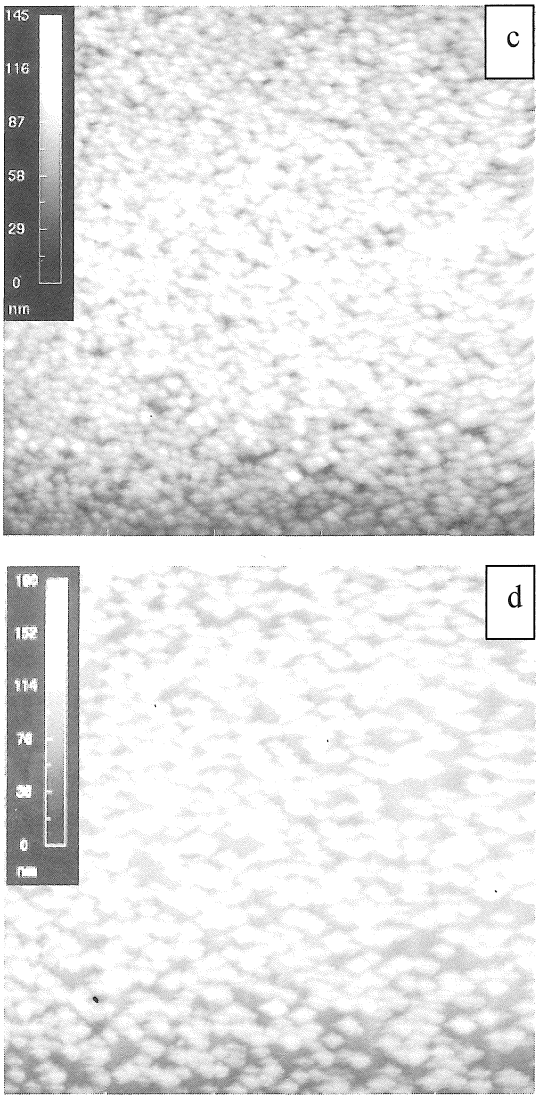

Figure 3. AFM images of the samples (a) 1#, (b) 7#, (c) 24#, and (d) M# (scan range is 10×10μm)

Figure 4. Amplified AFM image for the sample of 1#.

3.2 UV-vis Absorption Spectral Investigation

(1) Absorption spectra of glass/PVP$_d$-nanoAg monolayer films (1#, 7#, 24#)

Figure 5 shows the absorption spectra of Ag colloid and glass/PVP$_d$-nanoAg monolayer films (1#, 7#, 24#) as prepared, as well as those placed for 6 weeks in dark and at ambient environment. Only a few changes in absorption spectra were observed when the films were placed for a long time, suggesting that the obtained Ag colloidal films are stable in air and at room temperature. For the Ag colloid solution, the absorption peaks are broad with a main absorption at 445 nm due to dipole plasmon resonance, and two weak absorption shoulders at about 350 and 380 nm, attributed possibly to quadrupole plasmon resonance and wide size distribution[3]. In contrast, for the glass/PVP$_d$-nanoAg monolayer films, the main absorption peak generates dramatic blue-shift by 65 nm and a new absorption peak at long wavelength, which appears and becomes more clear when immerged for longer time in Ag colloid, can be seen. The blue-shift is due to the change in dielectric environment surrounding Ag nanoparticles from water (refractive index n_0=1.333) for the Ag colloid to air (n_0=1) for the glass/PVP$_d$-nanoAg films where the surrounding dielectric mediate also includes PVP layer. The effect of the surrounding dielectric environment on the plasmon resonance wavelength of spherical metal nanoparticles is easily understood using the plasmon resonance condition $\mathrm{Re}(\varepsilon_i)+2\varepsilon_0=0$, as described in the quasistatic approximation theory[3], where ε_i is the wavelength-dependent dielectric constant of the metal particle, $\varepsilon_0=n_0^2$ is the dielectric constant of the surrounding medium. Further derivation can obtain a qualitative equation:

$$\lambda_p=\lambda_{p,b}(2n_0^2+1)^{1/2}$$

Where λ_p is the plasmon resonance wavelength of metal particles, $\lambda_{p,b}$ the bulk plasmon resonance wavelength. From this equation, it is revealed that the plasmon wavelength varies roughly linearly with the refractive index of the surrounding medium. Therefore, the reduction of refractive index is responsible for the blue shift.

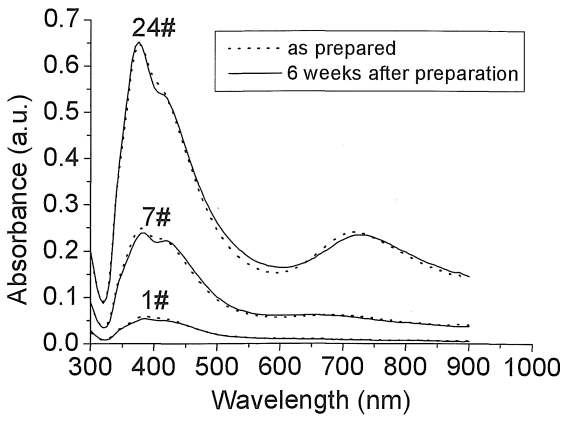

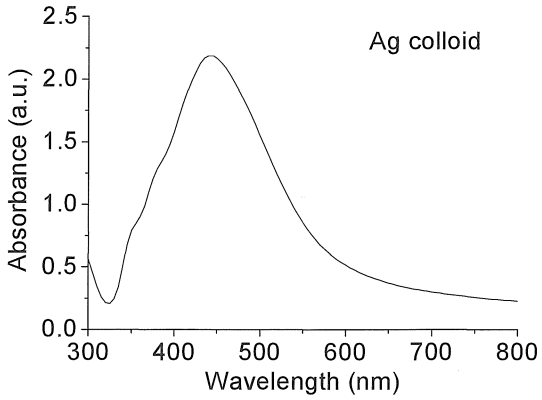

Figure 5. Absorption spectra for glass/(PVP$_d$-nanoAg)$_1$ monolayer films (1#, 7#, 24#) as prepared and placed for 6 weeks in dark and at ambient environment (upper). In contrast, the absorption spectrum of colloidal Ag solution aged for 6 days is also given below.

It is helpful for the generation of higher density of Ag nanoparticles in films (surface coverage) to increase the deposition time and the concentration of Ag colloid used[17,19]. Therefore, it is believed there is higher particle density for films of 7# and 24#, resulting in the existence of compact Ag nanoparticle aggregates which have been shown by the above AFM investigations. It has been demonstrated that the decrease of the separation between Ag nanoparticles in aggregates to a critical distance can result in a red-shifted and broadened plasmon peak at longer wavelength[17,20]. Therefore, the observed peaks in the range of 600-800nm for the samples of 7# and 24# can be attributed to a collective plasmon resonance or interparticle resonance[17]. The excitation of plasmon resonances leads to the oscillating local field surrounding Ag nanoparticles. The local field extends from the particle surface to a distance smaller than the wavelength of light (near field) and is enhanced as compared to the field of the incident light. When particles are closely spaced so that the local fields from individual particles overlap, the near field interaction takes place, and the system becomes coupled. This coupled system generates a new optical mode, termed collective plasmon oscillation in adjacent particles. In contrast, the absorption peaks in the range of 355-450nm are due to the plasmon resonance of isolated Ag nanoparticles or individual plasmon resonance, similar to that of dilute colloidal solution, although

the peak position produces a displacement because of the change in the dielectric environment as presented above. The collective surface plasmon resonance depends strongly on the interparticle distance and thus is sensitive to the Ag particle density in films. Therefore, the collective resonance peak appears, as well as becomes clear and red-shifts with increasing immerging time. For the film of 1#, even no collective resonance is observed due to the lower particle density, i.e., larger interparticle distance.

(2) Absorption spectra of glass/(PVP$_d$-nanoAg)$_n$ multilayer films (n=1-4)

The collective plasmon resonance was also observed for the glass/(PVP$_d$-nanoAg)$_n$ multilayer films (n=2-4) (Figure 6). Figure 7 also gives the linear dependence of the absorbance at 385 and 515 nm on the number of PVP$_d$-nanoAg bilayer. This linear dependence is a strong evidence of the formation of the multilayered structure in the films. The collective resonance is different from those discussed above for the monolayer film (called as intralayer collective resonance) and can be attributed to an interlayer collective resonance, because no collective resonance was observed for the case of n=1 where the immerging time was 1 hour (equivalent to 1#). We deduce that the interparticle distance (L) is too large in the Ag nanoparticle layer to generate the effective interparticle coupling, but the interparticle distance (D+t, t is the thickness of PVP$_d$ layer) is small enough to produce the strong collective resonance, as illustrated in figure8, where the PVP$_d$ layer thickness is estimated to be several nanometer which is sufficient to result in the interparticle resonance[17]

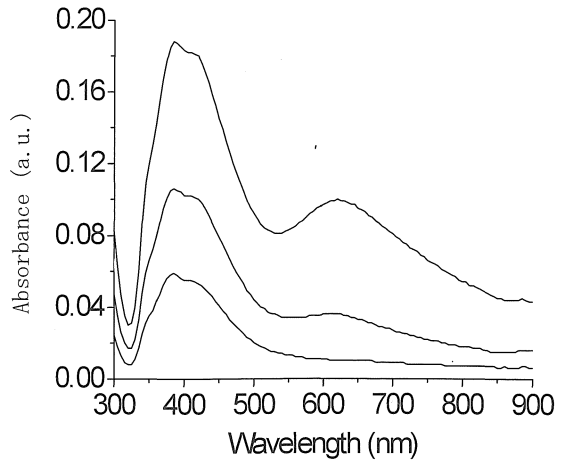

Figure 6. Absorption spectra of glass/(PVP$_d$-nanoAg)$_n$ multilayer films (n=1-4). From the lower to upper curves, the number of PVP$_d$-nanoAg bilayers is 1, 2, 3, and 4, respectively.

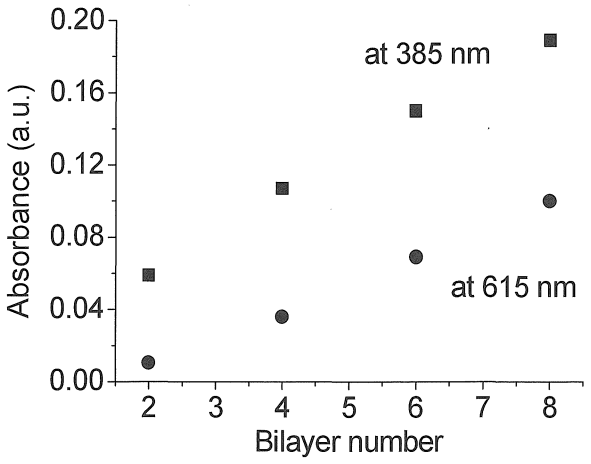

Figure 7. Absorbance at 385 nm and 615 nm as a function of the number of PVP$_d$-nanoAg bilayers.

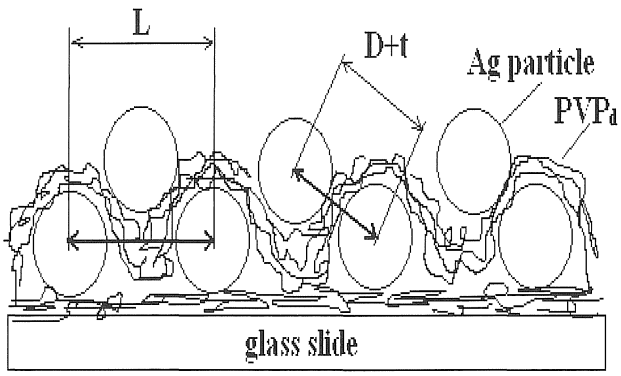

Figure 8. Structural schematics of the glass/(PVP$_d$-nanoAg)$_2$ multilayer film

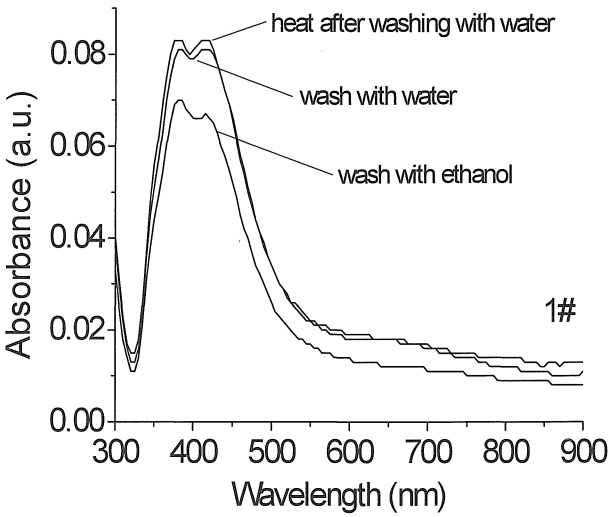

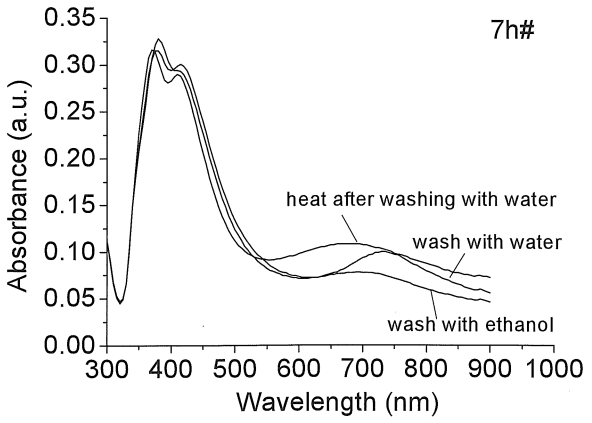

Figure 9. Absorption spectra for the samples 1#, 7#, and 24# at different post-treatment conditions: green and red line denotes the samples washed eventually with ethanol and water, respectively, and followed by drying at room temperature, black line denotes the samples washed eventually with water and followed by drying at 120℃ for 3 hours.

(3) Influence of different post-treatment conditions on Absorption spectra of glass/(PVP_d-nanoAg)$_1$ monolayer films (1#, 7#, 24#)

For the glass/(PVP_d-nanoAg)$_1$ monolayer films, different post-treatment processes, including drying from different solvents and heating at a higher temperature, are expected to affect on the interparticle resonance in the films due to the different particle aggregation states induced by the post-treatments. Upon drying, Ag nanoparticles underwent surface aggregation and the monolayer lost its uniformity. Two factors contribute to this aggregation[19]. First, the surface in the space between particles is covered with pyridyl groups that are not directly involved in the attachment of nanoparticles but can potentially interact with these. In the absence of electrostatic repulsion between particles, the interaction with these groups will result in the diffusion of nanoparticles on the surface. Second, drying reduces electrostatic repulsion and the surface tension of evaporating solvent layer forces nanoparticles to clump together. Figure 9 shows the absorption spectra of the samples 1#, 7#, and 24# under different post-treatment conditions. An explicit and uniform change in absorption band was observed for the collective plasmon resonance of all three samples when treated under different conditions. Obviously, this is related to the change in the interparticle aggregation states in the films induced by the solvent evaporation and heating process. Water has larger surface tension than ethanol and therefore induces more easily the formation of larger and more compact Ag particle aggregates which are responsible for the appearance of an absorption tail for 1# and the red-shift of the collective resonance for 7# and 24#, as shown by red curves. When the samples of 7# and 24# (washed eventually with water) were further heated at 120℃ for 3 hours, the collective resonance peaks became very broad. This is due to the strong interparticle coupling caused by heat-induced aggregation[4]. But for 1#, no obvious change in absorption band was observed. This is related to the lower density of nanoparticles in the film 1#.

4. Conclusions

Ag colloid self-assembled films (colloidal metal films) including monolayer (glass/(PVP_d-nanoAg)$_1$) and multilayer (glass/(PVP_d-nanoAg)$_n$) were fabricated by layer-by-layer self-assembly method, where PVP_d (poly(4-vinylpyridine)) was used to link metal nanoparticles by metal-ligand interactions. The obtained monolayer and multilayer films are optically stable at ambient environment, as demonstrated by absorption spectrum measurements. The plasmon resonance of isolated Ag nanoparticles (individual plasmon resonance) and collective plasmon resonance (interparticle plasmon resonance) were observed simultaneously for both mono- and multilayer films. And the intralayer collective resonance in the monolayer films and the interlayer collective resonance in the multilayer films have been investigated and distinguished experimentally. The influence of the post-treatment processes, including drying from different solvents and heating at a higher temperature, on the collective resonance was also evaluated. It is found that the heating treatment and washing with solvents of different surface tension is able to modify the collective resonance of Ag nanoparticles in the films.

References

1. U. Kreibig and M. Vollmer, *Optical Properties of Metal Clusters* (Springer, Berlin, 1995).
2. C. F. Bohren and D. R. Huffman, *Absorption and Scattering of Light by Small Particles* (Wiley, New York, 1983).
3. Kelly, K. L.; Coronado, E.; Zhao, L. L.; Schatz, G. C. *J. Phys. Chem. B* **2003**, *107*, 668.

4. Ung, T.; Liz-Marzan, L. M.; Mulvaney, P. *J. Phys. Chem. B* **2001**, *105*, 3441.
5. Mertens, H.; Verhoeven, J.; Polman, A.; Tichelaar, F. D. *Appl. Phys. Lett.* **2004**, *85*, 1317.
6. Fendler, J. H. *Chem. Mater.* **2001**, *13*, 3196.
7. Hutter, E.; Fendler, J. H.; Roy, D. *J. Phys. Chem. B* **2001**, *105*, 11159.
8. Caruso, F.; Spasova, M.; Salgueirin˜ o-Maceira, V.; Liz-Marza´n, L. *Adv. Mater.* **2001**, *13*, 1090. Westcott, S. L.; Oldenburg, S. J.; Lee, T. R.; Halas, N. J. *Langmuir* **1998**, *14*, 5396. Gittins, D. I.; Caruso, F. *J. Phys. Chem. B* **2001**, *105*, 6846.
9. Schmitt, J.; Decher, G.; Dressick, W. J.; Brandow, S. L.; Geer, R. E.; Shashidhar, R.; Calvert, J. M. *Adv. Mater.* **1997**, *9*, 61.
10. Sershen, S. R.; Westcott, S. L.; West, J. L.; Halas, N. J. *Appl. Phys. B* **2001**, *73*, 379.
11. Fu, Y.; Xu, H.; Bai, S.; Qiu, D.; Sun, J.; Wang, Z.; Zhang, X. *Macromol. Rapid Commun.* **2002**, *23*, 256.
12. Chen, S. *Langmuir* **2001**, *17*, 2878.
13. Huang, S.; Tsutsui, G.; Sakaue, H.; Shingubara, S.; Takahagi, T. *J. Vac. Sci. Technol., B* **2001**, *19*, 2045.
14. Wang, B.; Wang, H.; Li, H.; Zeng, C.; Hou, J. G.; Xiao, X. *Phys. Rev. B* **2000**, *63*, 035403.
15. He, J.-A.; Valluzzi, R.; Yang, K.; Dolukhanyan, T.; Sung, C.; water and dried Kumar, J.; Tripathy, S. K.; Samuelson, L.; Balogh, L.; Tomalia, D. A. *Chem. Mater.* **1999**, *11*, 3268.
16. Tsukruk, V. V.; Bliznyuk, V. N.; Visser, D. W.; Campbell, A. L.; Bunning, T.; Adams, W. W. *Macromolecules* **1997**, *30*, 6615.
17. Jiang, C. Y.; Markutsya, S.; Tsukruk, V. V. *Langmuir* **2004**, *20*, 882.
18. Lee, P. C.; Meisel, D. J. *Phys. Chem.* **1982**, *86*, 3391-3395.
19. Malynych, S.; Luzinov, I.; Chumanov, G. *J. Phys. Chem. B* **2002**, *106*, 1280.
20. Lazarides, A. A.; Schatz, G. C. *J. Phys. Chem. B* **2000**, *104*, 460.